Journal of the Korean Nuclear Society
Volume 33, Number 1, pp.25 ~ 33, February, 2001

Pin Power Reconstruction of HANARO Fuel Assembly via Gamma Scanning and Tomography Method

Chul Gyo Seo*, Chang Je Park, and Nam Zin Cho
Korea Advanced Institute of Science and Technology
373-1 Kusong-dong, Yusong-gu, Taejon, 305-701, Korea
cgseo@kaeri.re.kr

Hark Rho Kim
Korea Atomic Energy Research Institute
150 Dukjin-dong, Yusong-gu, Taejon, 305-353, Korea

(Received March 28, 2000)

Abstract

To determine the pin power distribution without disassembling, HANARO fuel assemblies are gamma-scanned and then the distribution is reconstructed by using the tomography method. The iterative least squares method (ILSM) and the wavelet singular value decomposition method (WSVD) are chosen to solve the problem. An optimal convergence criterion is used to stop the iteration algorithm to overcome the potential divergence in ILSM. WSVD gives better results than ILSM, and the average values from the two methods give the best results. The RMSE (root mean square errors) to the reference data are 5.1, 6.6, 5.0, 6.5, and 6.4% and the maximum relative errors are 10.2, 13.7, 12.2, 13.6, and 14.3%, respectively.

It is found that the effect of random positions of the pins is important. Although the effect can be accommodated by the iterative calculations simulating the random positions, the use of experimental equipment with a slit covering the whole range of the assembly horizontally is recommended to obtain more accurate results. We made a new apparatus using the results of this study and are conducting an experiment in order to obtain more accurate results.

Key Words : fuel, pin power reconstruction, gamma scanning, tomography.

1. Introduction

It is very important to accurately predict the pin power distribution in a reactor from the viewpoint of reactor safety as well as operability. The accuracy of the predictions must be verified against the measured data, which are obtained by the gamma scanning method. In order to measure the pin power distribution, it is inevitable to disassemble the assemblies. Assemblies used in

*Present Address: Korea Atomic Energy Research Institute

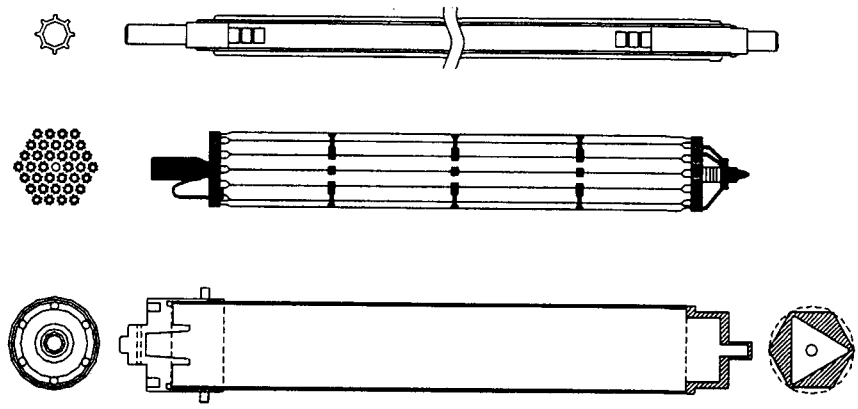

Fig. 1. Fuel Pin, 36-pin Assembly, and Al Canister

this measurement are almost fresh and clean from the viewpoint of burnup. The assembly is very expensive and it is very hard to reassemble it after disassembling. It takes a very long time to measure each pin individually. If it is possible to measure the pin power distribution without disassembling, we can save enormous time and cost. However, the adequacy of this method has not been fully proven yet, while that of the conventional method has been adequately validated and is used as a standard method. If this new method is proven to be proper, it can be widely applied to the validation of the pin power distribution. This paper introduces the experiment and some numerical studies to determine the pin power distribution from the assembly gamma scanning.

2. Experiment

During the nuclear commissioning of HANARO, the assemblies in a fresh and clean state were irradiated to measure the assembly power distribution and the fast flux distribution[1,2]. To activate the assemblies properly, the reactor was operated for about 16 hours at 150 kW. The assemblies were then cooled for 3 months and used to measure the radial and axial assembly power distributions by using the gamma scanning system at the IMEF (Irradiation Material Experimental Facility). The gamma scanning system, which can move the bench axially 0.01mm at a step and rotate 0.01° at a step, is very precisely controlled by a PLC (Programmable Logic Controller). In this experiment for the pin power distribution, an assembly is put into an Al canister filled with water to enlarge the attenuation differences of the gamma rays emitting from each pin. It is then located at the bench, which accepts a pin or an assembly, in the hotcell. Fig. 1 shows a pin, a 36-pin assembly, and an Al canister.

The assembly consists of 36 pins which are arranged in a hexagonal array with 1.2cm pin pitch. The active length of the fuel pin is 70cm. In the assembly, eighteen pins are arranged in the inner or middle hexagons and the others are located in the outer. The center position of the assembly is occupied by a central tie rod, which is made of zircaloy-4 and has the important role in keeping the shape and the mechanical integrity of the assembly in combination with the other structural components such as end plates and spacer plates. Pins are separated by three spacer plates. Fig. 2 shows the experimental schematics

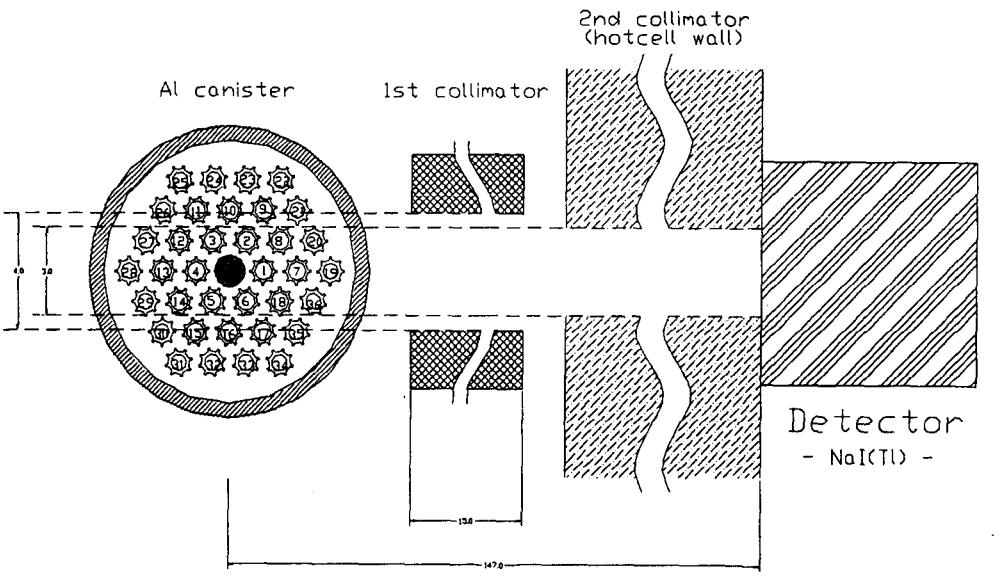

Fig. 2. Plan View of the Experimental Schematics

prepared for the experiment to measure gamma rays. In this experiment, the axial measuring position is at the axial peaking position of each assembly, namely a 2-dimensional measurement. The starting point of the axial measuring position can be determined easily because the shielding is nearly perfect and the axial movement is exactly controlled by PLC. The length of the pin is constant and the gamma rays from the fission products of the pins are observed only in the range. At the axial measuring position, the number of measuring positions are the number of pins to make a determinant problem as the assembly is rotating in steps of 10° in a counterclockwise direction.

To determine the angular starting point, a hexagonal shape at the lower part outside the Al canister, as in Fig. 1, is used. It turns out that this way is prone to inaccurate results, and some erroneous results are excluded after evaluating the measured data. The accuracy of the angular starting point cannot be evaluated quantitatively and the error is assumed to be within $\pm 1°$.

A HPGe (high purity germanium) detector is used to identify the nuclides before starting the gamma scanning, and then a NaI(Tl) detector is used to reduce the measuring time in all measurements. From the measurement using a HPGe detector, Zr-95 and Nb-95 were selected as the representative nuclides to measure the pin power distribution. Due to the low resolution of the NaI(Tl) detector, three peaks in the HPGe detector, which consist of 724.2(15%), 756.7(15%), and 765.8(70%) keV peaks[1,3], were overlapped and a summed peak were made in the NaI(Tl) detector.

Using a NaI(Tl) detector, the measurements to determine the pin power distribution were conducted for all sixteen 36-pin assemblies while rotating the assembly in 10° increments. After careful evaluation[4], 5 cases, i.e., the assemblies loaded at R04, R08, R09, R10, and R16 in the HANARO initial core, are used for this study, as in Fig. 3.

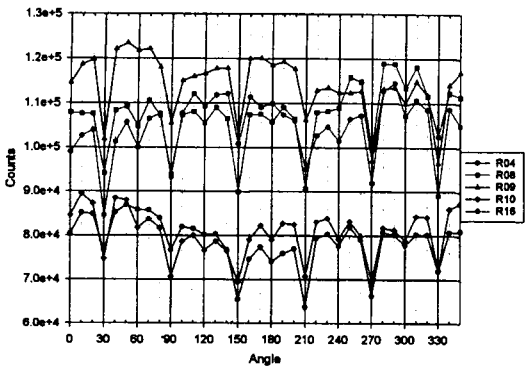

Fig. 3. Measured Counts - 5 Cases

3. Analysis

The gamma rays counted at a detector are the summation of the uncollided or not-attenuated gamma rays emitted from the pins in proportion to the pin power distribution. The pin power distribution $\boldsymbol{x} = \{x_1, x_2, \cdots, x_{36}\}$ and the measured counts $\boldsymbol{b}$ are related in a coupled set of equations as :

$$\sum_{i=1}^{36} a_{ij} x_i = b_j \quad \Rightarrow \quad \boldsymbol{Ax} = \boldsymbol{b}, \qquad (1)$$

where b_j, a_{ij}, and x_i represent the measured counts at angle j, the attenuation factor of pin i at angle j, and the power of pin i, respectively.

The attenuation factor a_{ij} means the possibility that a photon emitted from a pin i is detected at angle j. These factors can be obtained by calculation, but it is not easy to evaluate these factors accurately. Although this equation seems to be a simple linear algebraic equation, it is difficult to solve because it formally requires the inversion of matrix $\boldsymbol{A}$, which introduces some errors. This inverse problem is notorious for being poorly conditioned. The measured data $\boldsymbol{b}$ are insensitive to the variation of a single unknown x_i and small errors in $\boldsymbol{A}$ are magnified to large errors in $\boldsymbol{x}$. The accuracy of the pin power distribution is related to the accuracies of the measured results and the attenuation matrix, as follows[5] :

$$||\delta \boldsymbol{x}||/||\boldsymbol{x}|| \leq C_k(||\delta \boldsymbol{b}||/||\boldsymbol{b}|| + ||\delta \boldsymbol{A}||/||\boldsymbol{A}||), \qquad (2)$$

where the condition number C_k can be expressed in terms of norms of matrices as

$$C_k = ||\boldsymbol{A}||\,||\boldsymbol{A}^{-1}||. \qquad (3)$$

If we get exact $\boldsymbol{A}$ and $\boldsymbol{b}$, we can obtain the pin power distribution exactly. From the measurement, $\boldsymbol{b}$ is already obtained. To get the distribution $\boldsymbol{x}$, it is necessary to calculate the attenuation factor a_{ij}.

3.1. Calculation of Attenuation Factors

To calculate attenuation factors, we used the MCNP code, which can model complex geometry and has been validated to accurately solve various photon transport problems[6,7]. Fins at the cladding are approximated as cladding with an equivalent diameter because the directions of the fins are arbitrary. The source distribution in a pin might be important in the calculation of these factors, and usually the sources are mainly distributed at the outer portion of the pin due to the self-shielding effect. The source distribution is calculated using HELIOS[8], which is a lattice code that can model complex geometry. The source distribution is near flat because the fuel density (5.40g/cc) is not high and the fuel radius (0.3175cm) is small. The source distribution in the calculation of the attenuation factors is assumed to be flat and does not affect the results. Since the detector is far from the source (147cm) and uncollided photons are few, the calculation efficiency is very low. To overcome this difficulty in the calculation, the variance reduction technique is indispensable. The adopted variance reduction technique is source directional biasing[6], which makes the photons start mainly to a preferred direction and adjust their weight to have isotropic

source distributions equivalent to no biasing.

3.2. Numerical Methods

Several numerical methods were tried to solve this problem. Most methods give unrealistic results because both $\boldsymbol{A}$ and $\boldsymbol{b}$ have errors. In this kind of inverse problem, the iterative least squares method (ILSM) has been known to give good results[9] and the wavelet singular value decomposition method (WSVD)[4] has recently become popular [10,11].

ILSM is based on minimizing the relative difference R about a pin power $x_{i_o}^{n+1}$ between the measured counts b_j (with measurement error σ_j) and estimated counts c_j^n at the nth iteration in a least squares sense as follows[9] :

$$R(x_{i_o}^{n+1}) = \sum_j \frac{(b_j - c_j^n)^2}{\sigma_j^2} . \tag{4}$$

Solving for $x_{i_o}^{n+1}$, we get

$$x_{i_o}^{n+1} = x_{i_o}^n + \Delta^n x_{i_o} , \tag{5}$$

where $\Delta^n x_{i_o} = \left\{\sum_j a_{ji_o}[b_j - c_j^n]/\sigma_j^2\right\} / \sum_j (a_{ji_o}/\sigma_j)^2 .$

The solutions may not converge and could oscillate, so a damping factor δ is introduced. Again, using the least squares concept, we have the following equations :

$$x_{i_o}^{n+1} = x_{i_o}^n + \delta\Delta^n x_{i_o} , \tag{6}$$

where

$$\begin{aligned} \Delta^n x_{i_o} &= \left\{\sum_j a_{ji_o}[b_j - c_j^{n+1}]/\sigma_j^2\right\} / \sum_j (a_{ji_o}/\sigma_j)^2 , \\ c_j^{n+1} &= \sum_i a_{ij} x_i^n , \\ \delta &= \frac{\sum_j (b_j - c_j^n)\left[\sum_i a_{ji}\Delta^n x_i\right]/\sigma_j^2}{\sum_j \left(\sum_i a_{ij}\Delta^n x_i\right)^2/\sigma_j^2} . \end{aligned} \tag{7}$$

In WSVD, Eq. (1) is solved in the wavelet transformed domain.

We define the vectors :

$$\eta \equiv Wb, \quad \xi \equiv Wx . \tag{8}$$

where W is a matrix representation of the 1-D wavelet transform[12].

From Eqs. (1) and (8), we have

$$\eta = \Gamma \xi , \tag{9}$$

where the multiscale system matrix Γ is given by

$$\Gamma = WA W^T . \tag{10}$$

Using the regularized least squares (RLS), the solution of Eq. (9) is given by

$$(\Gamma^T\Gamma + \lambda I)\hat{\xi} = \Gamma^T\eta , \tag{11}$$

where λ is a regularization parameter.

Eq. (11) is then solved using the SVD method to overcome the near-singularity in matrix $\boldsymbol{A}$ (or Γ).

4. Results and Discussions

We do not have the measured pin power distribution yet, so the calculation results using MCNP are used as the reference data in this paper.

In case of no noise, the solutions by WSVD and ILSM are exact. Inherently, the measurement $\boldsymbol{b}$ and the attenuation matrix $\boldsymbol{A}$ have some noises. Unlike WSVD, ILSM converges to an unrealistic solution at a small noise. ILSM needs a stopping criterion to stop the iterations. The RMSE and discrepancy versus iterations are shown in Fig. 4. To stop the iteration properly, the discrepancy level is set to the same value for all cases[4]. The definition of RMSE in Fig. 4 is $[\sum_i(\hat{x}_i / x_i - 1)^2 / N]^{1/2} \times 100$ and that of discrepancy is $\sum_i | \hat{x}_i^{n+1} - \hat{x}_i^n |$.

As shown in Figs. 5~9, the reconstructed results have no peculiarity and are randomly distributed

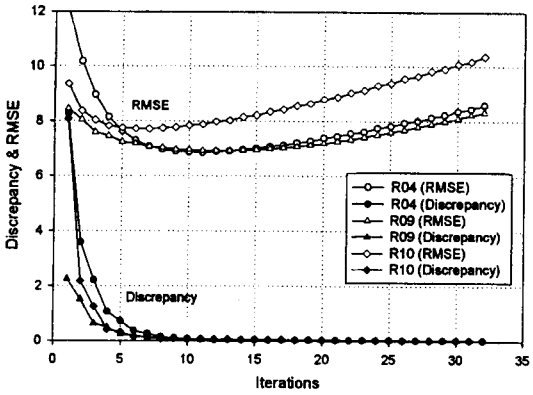

Fig. 4. The Divergence of the Solutions by ILSM

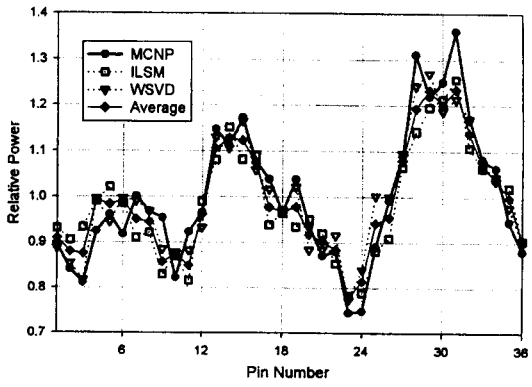

Fig. 5. Reconstructed Results of R04 Assembly

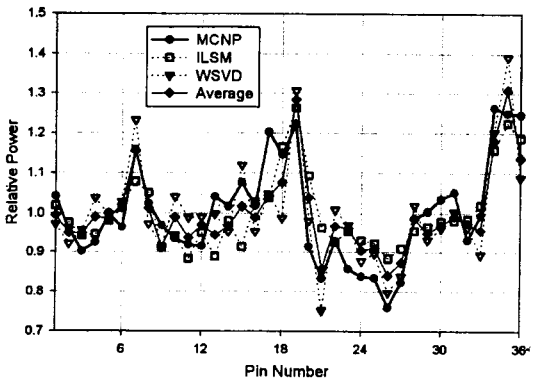

Fig. 6. Reconstructed Results of R08 Assembly

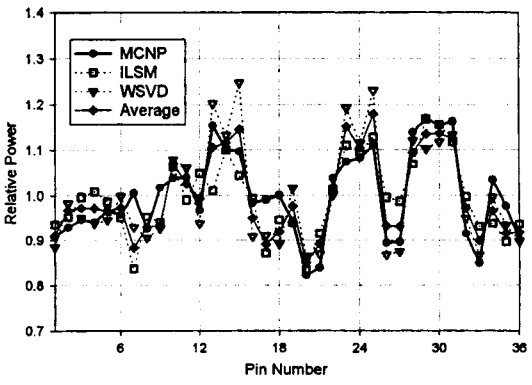

Fig. 7. Reconstructed Results of R09 Assembly

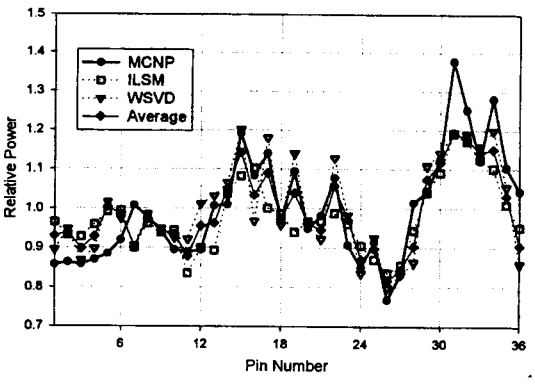

Fig. 8. Reconstructed Results of R10 Assembly

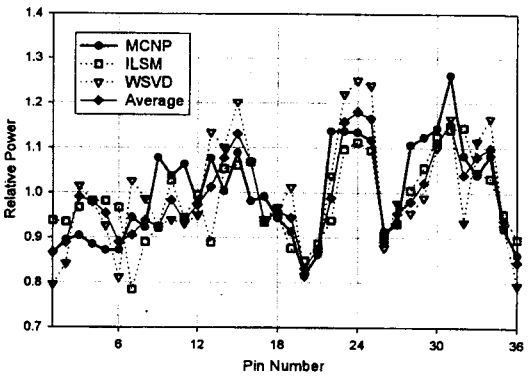

Fig. 9. Reconstructed Results of R16 Assembly

Table 1. Summarized Results Using WSVD and ILSM

Error / Case	RMSE(%)*			Maximum Relative Error(%)**		
	WSVD	ILSM	Average	WSVD	ILSM	Average
R04	4.90	6.89	5.13	12.48 at pin 25	15.06 at pin 3	-10.15 at pin 9
R08	7.87	8.25	6.61	-13.90 at pin 18	19.85 at pin 20	13.66 at pin 20
R09	5.71	6.72	4.98	13.66 at pin 15	-16.73 at pin 7	-12.15 at pin 7
R10	7.19	7.93	6.53	-17.67 at pin 9	-14.20 at pin 19	13.58 at pin 5
R16	8.57	7.98	6.44	-14.15 at pin 3	-17.55 at pin 22	-14.30 at pin 9

* RMSE(%) : $[\sum_i^N (\hat{x}_i / x_i - 1)^2 / N]^{1/2} \times 100$

** Maximum Relative Error(%) : $\pm$ max $| \hat{x}_i / x_i - 1 | \times 100$

about the reference data. The average value at pin i, $\overline{x_i}$, is chosen as $(x_i^{ILSM} + x_i^{WSVD}) / 2$ of x_i^{ILSM} from ILSM and x_i^{WSVD} from WSVD at pin i. The errors are almost below 10% and the positions of the maximum errors are different.

The reconstructed results are summarized by showing RMSE and Maximum Relatvie Error in Table 1. WSVD gives slightly better results and is more stable than ILSM. The average values from these two methods could be used as the two methods are independent. Considering that the reference data have a statistical error of 3%[1], the reconstructed results would be close to the real distribution.

The divergence of the solutions by ILSM, and the errors by ILSM and WSVD, come from errors in the attenuation factors. This is inferred from the fact that the calculated results are always lower than the measured results at every position having lower counts in Fig. 10. The attenuation factors are calculated assuming that the pins are in position as designed. In practice, the pins are not exactly seated at the design position but randomly

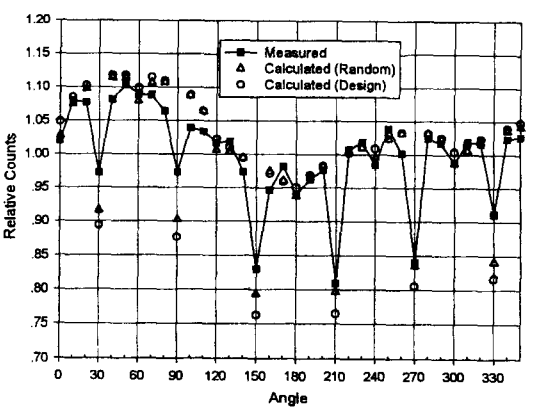

Fig. 10. Effects by a Random Positions of the Pins

positioned about the design position with an engineering tolerance. Although the pins are well positioned within the tolerance, the attenuation factors are affected by a small deviation. The attenuation factors at the positions having lower counts become large because the photons of the pins that deviate from the design position are no longer attenuated by the pins. The locations of pins in the MCNP model are simulated by

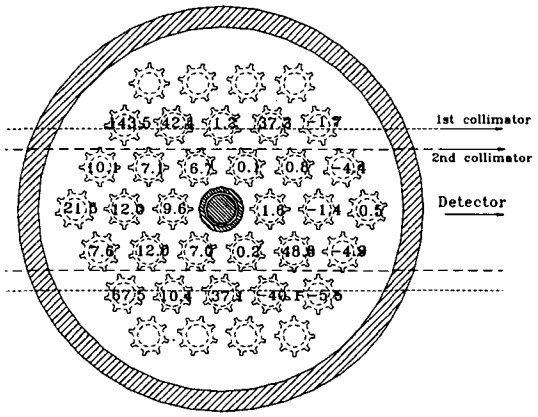

Fig. 11. Relative Differences of the Attenuation Factors by Random Positions

generating random numbers with a Gaussian distribution about the design position. The maximum deviation from the design position is selected to a certain value, 0.15cm, from the evaluation of the manufacturer. A lot of calculations are needed to reasonably simulate the effect of a random pin position. Because the expected computing time is very long, only a set of the MCNP calculations are performed to study the effect. The calculated $\boldsymbol{b}^R=\boldsymbol{A}^R\boldsymbol{x}^c$, by the attenuation matrix, $\boldsymbol{A}^R$, calculated using the random positions of the pins and the pin power distribution $\boldsymbol{x}^c$ from the reactor calculation are compared with the measurement $\boldsymbol{b}$ at R04 assembly in Fig. 10.

As expected, the measured $\boldsymbol{b}$ and the calculated $\boldsymbol{b}^R$ by consideration of the random positions agree better than the calculated $\boldsymbol{b}^D=\boldsymbol{A}\boldsymbol{x}^c$ by the design positions. Because random positions of the pins are not fully implemented, the improvement in the reconstructed results is not remarkable.

The relative differences between the attenuation factors by the design positions and by the random positions are provided and are very large at the pins near the extended lines of slit as in Fig. 11. This indicates that the random positions of the pins much significantly affect the attenuation factors at the pins near the extended lines of slit, which means that the accuracy of slit width is very important. It is possible to reduce the effect of a random pin position on the attenuation factor, although there exists a limitation in enhancing the precision of slit width. Thus, the insufficient coverage of the present narrow slit with precision not good enough may result in deteriorating the accuracy of the reconstructed results. Therefore, it would be better to measure with a wide slit enough to fully cover the assembly horizontally.

5. Concluding Remarks

HANARO fuel assemblies are gamma-scanned to determine the pin power distribution nondestructively and then the distribution is reconstructed by using two numerical methods. The two methods are useful to solve the problem; WSVD gives better results than ILSM, and the average values from the two methods give the best results.

Although the reconstructed results are not so accurate, this study suggests a possibility that the pin power distribution can be determined nondestructively. To get more accurate results, the effect of random positions of the pins must be properly considered. Two proposals are presented. One is to take account of the random positions in the calculation of the attenuation factors. Another is to make new measuring equipment with a wider slit.

We prepared a new apparatus using the results of this study and established a measuring strategy to get better results. The pin power distribution after disassembling several assemblies will be measured to confirm the numerical solutions.

Acknowledgement

This work was performed with the support of

the Ministry of Science and Technology of Korea and appreciation is expressed for the sponsorship.

References

1. Chul Gyo Seo, " Assemblywise Power Distribution Measurement," *HANARO Commissioning Test Report, TP-RPT-C-08*, Korea Atomic Energy Research Institute (1998).
2. Byung Chul Lee and Chul Gyo Seo, "Thermal and Fast Neutron Reaction Rates in HANARO," *Proc. of the 5th Asian Symposium on Research Reactors*, **1**, 117, Taejon, Korea, May 29-31 (1996).
3. Chul Gyo Seo, et al., " Pin Power Reconstruction from the HANARO Fuel Assembly Gamma Scanning," *Proc. of the Korean Nuclear Society Autumn Meeting*, Seoul, Korea, Oct. (1998).
4. Chul Gyo Seo, "Reconstruction of the Pin Power Distribution from the HANARO Fuel Assembly Gamma Scanning," MS Thesis, Korea Advanced Institute of Science and Technology, Feb. (1999).
5. N. J. McCormick, "Inverse Radiative Transfer Problems: A Review," *Nucl. Sci. Eng.*, **112**, 185 (1992).
6. J. F. Briesmeister (Editor), "MCNP-A General Monte Carlo N-Particle Transport Code," LA-12625-M, Los Alamos National Lab. (1993).
7. D. J. Whalen, et al., "MCNP: Photon Benchmark Problems," LA-12196 (1991).
8. Eduardo A. Villarino, et al., "HELIOS: Angularly Dependent Collision Probabilities," *Nucl. Sci. Eng.*, **112**, 16 (1992).
9. T. F. Budinger and G. T. Gullberg, "Three-Dimensional Reconstruction in Nuclear Medicine Emission Imaging," *IEEE Trans. Nucl. Sci.*, NS-21, 2 (1974).
10. N.Z. Cho and C.J. Park, "A Wavelet-Based Image Reconstruction in Transmission Computed Tomography," *Proc. of 1998 ANS Radiation Protection and Shielding Division Topical Conference*, **2**, 141, Nashville, U.S.A., Apr. (1998).
11. C.J. Park and N.Z. Cho, " Image Reconstruction in Emission Computed Tomography via Multigrid Wavelet-Based Natural Pixel Method," *Proc. Int. Conf. on the Physics of Nuclear Science and Technology*, Long Island, New York, Oct. (1998).
12. G. Beylkin, et al., "Fast Wavelet Transforms and Numerical Algorithms," *Comm. Pure. Appl. Math.*, **43**, 141 (1991).